Synergy of Electron-Cyclotron and Lower-Hybrid Current Drive in Steady-State Plasmas

G. Giruzzi, J. F. Artaud, R. J. Dumont, F. Imbeaux, P. Bibet, G. Berger-By, F. Bouquey, J. Clary, C. Darbos, A. Ekedahl, G. T. Hoang, M. Lennholm, P. Maget, R. Magne, and J. L. Ségui

Association Euratom-CEA, CEA/DSM/DRFC, CEA/Cadarache, 13108 St. Paul-lez-Durance, France

A. Bruschi and G. Granucci

Associazione Euratom-ENEA-CNR, IFP-CNR, Milano, Italy

(Received 12 July 2004; published 15 December 2004)

Improvement (up to a factor of ~4) of the electron-cyclotron (EC) current drive efficiency in plasmas sustained by lower-hybrid (LH) current drive has been demonstrated in stationary conditions on the Tore Supra tokamak. This was made possible by feedback controlled discharges at zero loop voltage, constant plasma current, and constant density. This effect, predicted by kinetic theory, results from a favorable interplay of the velocity space diffusions induced by the two waves: the EC wave pulling low-energy electrons out of the Maxwellian bulk, and the LH wave driving them to high parallel velocities.

DOI: 10.1103/PhysRevLett.93.255002 PACS numbers: 52.50.Sw, 52.55.Wq

Noninductive current drive (CD) [1] has two main applications in tokamaks: sustainment of a substantial fraction of the toroidal current necessary for the plasma confinement, and control of the plasma stability and transport properties by appropriate shaping of the current density profile. For the first kind of applications, lower-hybrid (LH) waves are known to provide the highest efficiency (defined as the ratio of the driven current to the injected wave power), although with limited control capability. Conversely, electron-cyclotron (EC) waves drive highly localized currents, and are therefore particularly suited for control purposes, but their CD efficiency is much lower than that of LH waves (typically, an order of magnitude in present day experiments, but the same order of magnitude at reactor relevant temperature). The reason for this difference is related to the different interaction mechanisms of the two waves with the electrons: parallel velocity diffusion associated with Landau damping for LH waves and perpendicular velocity diffusion associated with cyclotron damping for EC waves (parallel and perpendicular directions are defined with respect to the equilibrium magnetic field). LH waves can efficiently drive electrons from low to substantially higher parallel velocities, making them poorly collisional and insensitive to trapping, thus carrying a larger current than the slower electrons interacting with the EC waves. For these reasons, the idea of combining the two CD systems has been proposed and investigated since the early 1980s [2] and has stimulated dedicated experiments on the WT-2 [3,4], JFT-2M [5,6], and WT-3 [7,8] tokamaks. Moreover, kinetic calculations [9] performed with a 3D Fokker-Planck code have numerically demonstrated an interesting property: the current driven by the simultaneous use of the two waves, $I_{\mathrm{LH+EC}}$, can be significantly larger than the sum of the currents separately driven by the two waves, $I_{\mathrm{LH}} + I_{\mathrm{EC}}$, in the same plasma conditions. This property, hereafter called the synergy effect, has been subsequently confirmed by a different Fokker-Planck code [10], by a self-consistent kinetic-transport code [11], and by analytical calculations [12]. The above-mentioned experiments [3–8] have shown that EC waves could couple to the fast electron tail sustained by LH waves and thus provide efficient current ramp-up, despite the fact that in most cases the EC waves absorption took place after multiple reflections on the tokamak walls. However, it is well known [1] that the physics of current ramp-up is dominated by the inductive response of the plasma, i.e., the transient reverse electric field, and not simply by the kinetic balance of quasilinear wave diffusion and Coulomb collisions. Mainly for this reason, these experiments could not provide a qualitative and quantitative assessment of the synergy effect. Demonstration of the synergy effect has thus been attempted in stationary conditions (i.e., at constant plasma current I_p) on Versator II [13] and on TdeV [14], but the results of these two experiments were inconclusive, or even negative, mainly because of the poor confinement of superthermal electrons. Effective coupling of EC waves with the LH driven electron tail has been observed on the Frascati tokamak upgrade [15], providing qualitative indications on a possible ECCD efficiency improvement. In this Letter, the first experimental demonstration of the synergy effect in steady state is reported.

An unambiguous experimental demonstration of the synergy effect requires (1) stationary conditions, i.e., constant I_p, constant density, and no substantial electric field effects, (2) good confinement of the current carrying electrons, and (3) large optical depth for the EC waves. If all these conditions are met, not only a qualitative assessment, but also a quantitative comparison with the CD improvement predicted by kinetic theory, is possible. Dedicated experiments have been performed in the Tore Supra tokamak (major radius $R = 2.40$ m, minor radius $a = 0.72$ m, magnetic field $B \approx 3.8$ T, circular cross section). Discharges of a duration of 30 s have been realized in deuterium, at a plasma current $I_p = 0.58$ MA, central electron density $n_{e0} \approx 1.8 \times 10^{19}$ m^{-3}, central electron and ion temperatures $T_{e0} \approx 6$–8 keV, $T_{i0} \approx 1.7$ keV, and

effective ion charge $Z_{\text{eff}} \approx 4$. After an initial Ohmic phase, the transformer flux was kept constant and the plasma current was sustained by LH waves, launched by two couplers with power spectra peaked at $n_{||} \approx 2$ and a total power $P_{\text{LH}} \approx 3$ MW, at a frequency of 3.7 GHz. The calculated bootstrap current contribution was of the order of $I_{\text{bs}}/I_p = 10\%$–15%. A multiple feedback strategy was employed, with the following actuators: (1) a gas puff to keep the plasma density constant, (2) LH power to keep the plasma current constant, and (3) transformer flux to keep the loop voltage V_{loop} constant and exactly equal to zero. On the stationary phase of this target plasma, EC waves have been injected for a duration of 10 s. Two gyrotrons [16] at 118 GHz have been used to inject a total power $P_{\text{EC}} \approx 0.7$ MW into the plasma in the ordinary mode (1st harmonic), by means of poloidally and toroidally steerable mirrors. During the ECCD phase, the LH power is expected to drop by an amount ΔP_{LH}, because the plasma current is kept constant. Since the loop voltage is zero, this drop is easily translated into the corresponding additional current ΔI, driven by the EC waves in the presence of LH waves, by the formula

$$\Delta I = (I_p - I_{\text{bs}}) \frac{\Delta P_{\text{LH}}}{P_{\text{LH}}}. \quad (1)$$

The relationship between ΔI and ΔP_{LH} can be expressed in this simple form provided the bootstrap current and the LH efficiency vary little in the relevant phases of the discharge, which is the case for these experiments. Otherwise, Eq. (1) has to be corrected for these and other variations (e.g., Z_{eff}). The current ΔI is then compared to the current I_{EC} that would be driven by ECCD alone in the same plasma conditions, which can be evaluated by means of standard toroidal ray-tracing codes, coupled to a Fokker-Planck code or, more simply, to linear expressions of the current drive efficiency [17], which is completely appropriate to this power level. These theoretical expressions have been fully validated by a dedicated series of experiments, performed on the DIII-D tokamak in a variety of different plasma conditions [18–20]: they can be used as a reliable reference for the ECCD efficiency in conditions of strong single pass absorption and good confinement of the current carrying electrons. The synergy effect can be quantified, e.g., by the synergy factor [11] defined as $F_{\text{syn}} = \Delta I/I_{\text{EC}}$, where $\Delta I = I_{\text{LH+EC}} - I_{\text{LH}}$.

The results obtained are well illustrated by the time history of discharge 31 463, shown in Fig. 1. During the application of ECCD ($P_{\text{EC}} \approx 0.7$ MW), the LH power drops by approximately $\Delta P_{\text{LH}} \approx 0.5$ MW, at constant transformer flux, plasma current, and density. This simple experimental fact implies that the additional current driven by the ECCD has an efficiency of the same order of magnitude as LHCD. Application of Eq. (1), with a computed bootstrap current $I_{\text{bs}} \approx 80$ kA, yields $\Delta I \approx 90$ kA, to be compared with the linear estimate $I_{\text{EC}} \approx 24$ kA. In

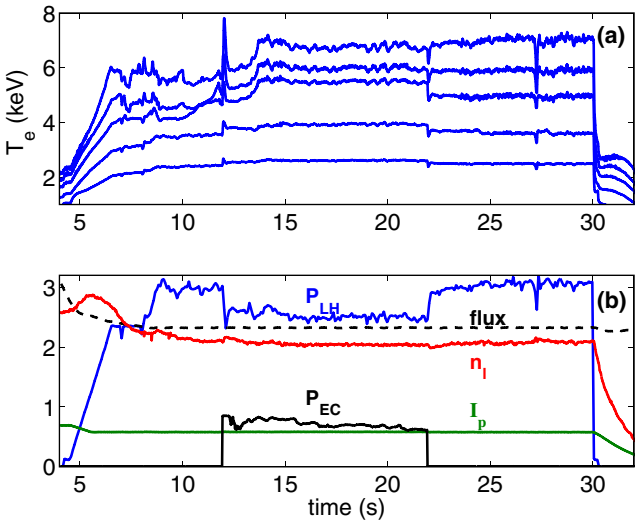

FIG. 1 (color online). Tore Supra discharge 31 463. (a) Electron temperature measured by electron cyclotron emission (ECE) at various positions, covering the region $0 \le r/a \le 0.4$. (b) From top to bottom: as a function of time, LH power (MW), transformer flux (W b), line integrated density (10^{19} m^{-2}), EC power (MW), and plasma current (MA).

this case, the toroidal injection angles of the two EC wave beams were 24° ($n_{||} \approx 0.5$ at the absorption point), and the poloidal injection angles had been chosen in order to drive a current peaked at the same location as the LH driven current. The large drop of ΔP_{LH} in the ECCD phase cannot be explained by an increase of the LHCD efficiency due to the temperature increase. In fact, the LHCD efficiency on Tore Supra is found to increase weakly with the temperature (a square root dependence) and the average temperature variation between the ECCD and the post-ECCD phases is less than 5%. Note that this temperature difference before and after the ECCD phase is due to a change in the confinement properties of the discharge, related to a corresponding modification of the q profile. This little change of the T_e profile also explains why the bootstrap

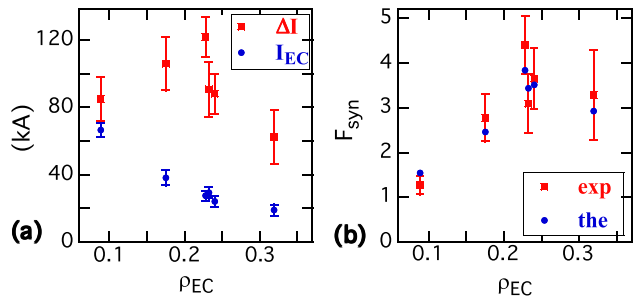

FIG. 2 (color online). (a) Measured additional current by ECCD in the presence of LHCD (squares) and computed ECCD current (circles) versus the location ρ_{EC} (in normalized radius) of maximum EC power deposition. (b) Synergy factors from experiment (squares) and from kinetic theory (circles) versus ρ_{EC}.

current changes little. Measured variations of the LH wave coupling are also $<3\%$, meaning that the variation in LH spectrum directivity, and therefore current drive efficiency, was small. Therefore, the synergy effect remains the most plausible explanation of the ECCD efficiency improvement.

The radial location ρ_{EC} at which the EC current is driven has then been varied by changing the poloidal and toroidal launch angles, and it has been observed that the synergy effect depends on this location. The measured additional currents ΔI and the linear ECCD currents I_{EC} are shown in Fig. 2(a) versus ρ_{EC} (radial coordinate, normalized to the plasma minor radius, determined by ray-racing calculations). The error bars of ΔI correspond to the standard deviation associated with the statistical variations of P_{LH} and I_{bs} (calculated from the measured plasma parameters by means of the NCLASS code [21]) in the time intervals chosen for the analysis. The error bars of I_{EC} also correspond to statistical variations of the measured plasma parameters and, in addition, to the uncertainty on the injection angles ($\pm 1°$, typically). The estimate of ΔI can be corrected by smaller effects due to other parameters (slight I_p, n_e, and Z_{eff} variations, transient Ohmic current, weak dependence of I_{LH} on T_e and P_{LH}, and LH coupling variation during the ECCD phase). These corrections moderately affect the mean value of ΔI and of its error bar, but do not change the overall conclusion: ΔI is always larger than I_{EC}.

In order to understand the dependence of ΔI on ρ_{EC} (or on the launching angles), kinetic simulations of the discharges presented in Fig. 2(a) have been performed, using a 3D relativistic Fokker-Planck code [22], and focusing the comparison on the synergy factor F_{syn}. The measured temperature and density profiles as well as other experimental parameters are used as an input to the Fokker-Planck code. The EC wave beams propagation is described by tracing 150 rays per beam and summing up all the contributions to the quasilinear diffusion coefficient. The result of the comparison of the synergy factors for the discharges of Fig. 2(a) is shown in Fig. 2(b). The overall behavior of $F_{\mathrm{syn}}(\rho_{\mathrm{EC}})$ is well reproduced, in particular, the strong reduction for central EC power deposition. As explained later on, this is related to the different values of $T_e(\rho_{\mathrm{EC}})$ and to the different conditions of overlap in velocity space of the two interactions [12].

The physical origin of the synergy effect can be better understood by plotting quantities proportional to the nonthermal power absorption patterns of the two waves in velocity space, i.e.,

$$p_{\mathrm{LH}} = -D_{\mathrm{LH}} u_{\|} \frac{\partial f_{\mathrm{nM}}}{\partial u_{\|}}, \qquad p_{\mathrm{EC}} = -D_{\mathrm{EC}} u_{\perp} \frac{\partial f_{\mathrm{nM}}}{\partial u_{\perp}}, \quad (2)$$

where D_{LH} and D_{EC} are the quasilinear diffusion coefficients associated with the two wave spectra, $f_{\mathrm{nM}} = f - f_{\mathrm{M}}$ is the non-Maxwellian part of the electron distribution function, and $u_{\perp}$ and $u_{\|}$ are momentum components normalized to $(m_e T_{e0})^{1/2}$. Color contour plots of p_{EC} and p_{LH} (normalized to their maximum values), computed for the parameters of one of the experimental discharges, with EC and LH waves alone are shown in Figs. 3(a) and 3(b), respectively. The sum of the normalized p_{EC} and p_{LH} for a simulation with both waves is shown in Fig. 3(c). It clearly appears that the effect of the EC waves is to push electrons to higher $u_{\perp}$ and $u_{\|}$ (from the blue to the red spot), thus allowing them to reach, with the help of collisional pitch-angle scattering, the low $u_{\|}$ and high $u_{\perp}$ limit of the LH interaction region. As a consequence, at all LH-resonant $u_{\|}$ values, p_{LH} is extended to higher perpendicular velocities, from where the synergy current originates.

Another way to visualize the synergy mechanism is through the relaxation of electrons subject to the stochastic force terms associated with Coulomb collisions and quasilinear diffusion [12]. Examples of electron trajectories, computed by a code solving the appropriate Langevin equations [12], are shown in Fig. 4. The case of Fig. 4(a) corresponds to the absorption patterns of Fig. 3. An electron representative of those excited by the EC waves, i.e., originating from the red spot of Fig. 3(a) ($u_{\perp} \approx 2, u_{\|} \approx 3$), carries current during its relaxation, which can be strongly influenced by the presence of the LH waves (red trajectory), with respect to the purely collisional one (blue trajectory). This electron starts its relaxation in a region

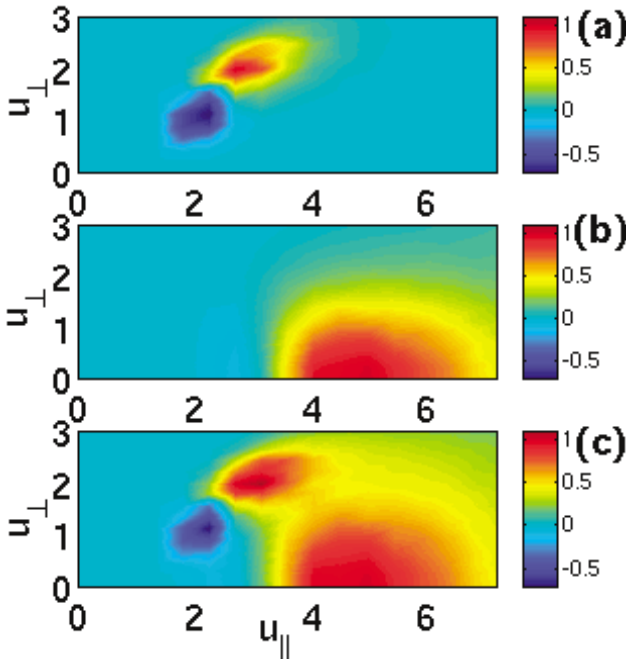

FIG. 3 (color). Normalized nonthermal power absorption patterns in momentum space, from the kinetic simulation of discharge 31 506, at $\rho \approx 0.14$. (a) EC only; (b) LH only; (c) LH + EC.

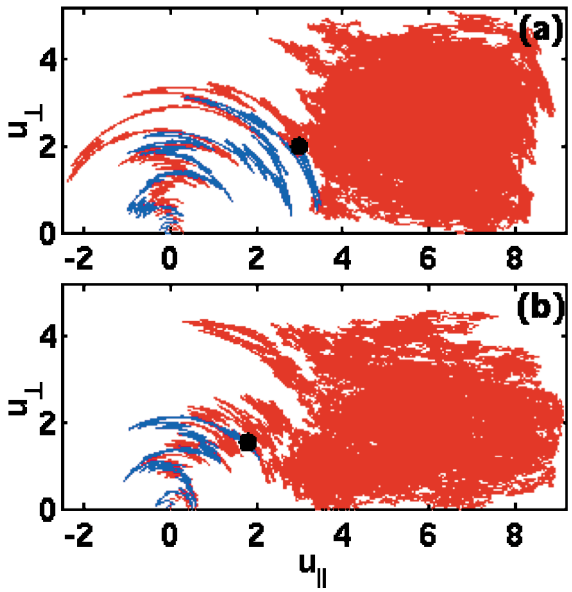

FIG. 4 (color). Electron trajectories computed from the Langevin equations (black circles are the initial conditions). Purely collisional relaxation (blue) and collisional relaxation in the presence of LH (red). (a) Discharge 31 506, corresponding to a moderate synergy factor ($F_{\mathrm{syn}} \sim 1.5$). (b) Discharge 31 463, high synergy factor ($F_{\mathrm{syn}} \sim 3.5$).

of vanishing LH power [see Fig. 3(b)]; nevertheless, it has a finite probability to enter the LH region by collisional pitch-angle scattering and to spend a long time there, carrying a substantial additional current. This corresponds to a case of moderate synergy ($\rho_{\mathrm{EC}} \sim 0.14$). A case of higher synergy factor ($\rho_{\mathrm{EC}} \sim 0.23$) is shown in Fig. 4(b). In this case the EC absorption takes place at a lower temperature; thus the EC interaction pattern is maximum at a lower velocity ($u_\perp \approx 1.5$, $u_\parallel \approx 1.8$). The collisional relaxation trajectory (blue) is now much shorter, which corresponds to a much lower driven current. In contrast, the relaxation trajectory in the presence of LH (red) is very similar to that of Fig. 4(a), as well as the additional driven current. These features, although qualitative, clarify what is the main effect of LH waves on ECCD: that of making the ECCD efficiency much less sensitive to T_e, i.e., to the interaction location in velocity space. This is also apparent in Fig. 2: the variations of ΔI with ρ_{EC} are much weaker that those of I_{EC}. The effect on trapping is qualitatively similar, although quantitatively less relevant for the parameters of these experiments.

In conclusion, the experimental conditions attainable on the Tore Supra tokamak have allowed the first experimental demonstration of the synergy between the EC and LH current drives. Comparison of the experimental results with kinetic theory shows systematic agreement on a so far limited base of discharges. The use of LH waves in combination with EC waves acts on the most basic phenomena that limit the ECCD efficiency: the strong sensitivity to temperature and to trapping. Therefore, this effect may find its most useful application in off-axis current profile control. A synergy factor in the range 2–4 implies a significant improvement in the control capability of EC waves, if used in conjunction with LH waves. This opens up the possibility of developing new plasma scenarios, including sustainment of transport barriers in steady state and stabilization of MHD phenomena with substantially reduced EC power requirements.

The diligent support of the Tore Supra Team is gratefully acknowledged, as well as continuous support and encouragement by Dr. I. Fidone, who is at the origin of this work.

[1] N. J. Fisch, Rev. Mod. Phys. **59**, 175 (1987).
[2] I. Fidone *et al.*, Phys. Fluids **27**, 2468 (1984).
[3] A. Ando *et al.*, Phys. Rev. Lett. **56**, 2180 (1986).
[4] A. Ando *et al.*, Nucl. Fusion **26**, 107 (1986).
[5] T. Yamamoto *et al.*, Phys. Rev. Lett. **58**, 2220 (1987).
[6] H. Kawashima *et al.*, Nucl. Fusion **31**, 495 (1991).
[7] T. Maekawa *et al.*, Phys. Rev. Lett. **70**, 2561 (1993).
[8] T. Maehara *et al.*, Nucl. Fusion **38**, 39 (1998).
[9] I. Fidone *et al.*, Nucl. Fusion **27**, 579 (1987).
[10] M. Shoucri *et al.*, Comput. Phys. Commun. **55**, 253 (1989).
[11] R. J. Dumont, G. Giruzzi, and E. Barbato, Phys. Plasmas **7**, 4972 (2000).
[12] R. J. Dumont and G. Giruzzi, Phys. Plasmas **11**, 3449 (2004).
[13] J. A. Colborn *et al.*, Nucl. Fusion **38**, 783 (1998).
[14] C. Côté *et al.*, in *1998 ICCP and 25th EPS Conference on Controlled Fusion and Plasma Physics, Praha, 1998*, edited by P. Pavlo (European Physical Society, Petit-Lancy, 1998), Vol. 22C, p. 1336.
[15] G. Granucci *et al.*, in *Proceedings of the 12th Joint Workshop on ECE and ECRH, Aix-en-Provence, 2002*, edited by G. Giruzzi (World Scientific, Singapore, 2003), p. 341.
[16] M. Lennholm *et al.*, Nucl. Fusion **43**, 1458 (2003).
[17] R. H. Cohen, Phys. Fluids **30**, 2442 (1987).
[18] R. A. James *et al.*, Phys. Rev. A **45**, 8783 (1992).
[19] C. C. Petty *et al.*, Nucl. Fusion **42**, 1366 (2002).
[20] C. C. Petty *et al.*, Nucl. Fusion **43**, 700 (2003).
[21] W. A. Houlberg *et al.*, Phys. Plasmas **4**, 3230 (1997).
[22] G. Giruzzi, Plasma Phys. Controlled Fusion **35**, A123 (1993).